Investigation of the aerosol component of the atmosphere by means of measurements of scattering coefficients of light

SYLWESTER PUCHALSKI

Institute of Geophysics, Polish Academy of Sciences, ul. Księcia Janusza 64, 01–452 Warszawa, Poland.

Results are presented of aerosol extinction coefficient measurements in air layers over ground and water $\alpha_A(\lambda)$ at wavelength $\lambda \in (380, 1100 \text{ nm})$ made by means of the multi-channel transmission meters at Belsk Geophysical Observation (BGO) and in Gdynia, Poland, as well as the results of vertical aerosol optical thickness measurements $\tau_A(\lambda)$ at $\lambda \in (380, 667 \text{ nm})$ made by means of Linke's radiometer at BGO and aerosol back-scattering coefficients profiles in the stratosphere: $\beta_A(\lambda = 532 \text{ nm})$ and $\beta_A(\lambda = 1064 \text{ nm})$ made at BGO and Institute of Physics in Minsk (Byelorussia) by means of lidar. On the basis of these measurements, we determined, by using randomized minimization search technique (RMST) and bimodal log-normal model of the aerosol, the following parameters: particle number density concentration N, particle volume concentration V, mean modal radius a_{mm} and effective particle radius a_{eff} of the atmospheric aerosols. It was found that during the last few years (1992−1998) "cleaning of the atmosphere" over Poland took place and the transformation of aerosol towards the smaller particles (there was observed a decrease of V − proportional to the weight concentration, a decrease of a_{mm} and a_{eff}, along with an increase of N).

1. Introduction

The atmosphere is a turbid medium in which light, in visible and near infrared range, is attenuated, chiefly by scattering. The light scattering in a turbid medium is due to fluctuation of refractive index. The fluctuations in the atmosphere are produced by air molecules, aerosols and elements of clouds and precipitation. Atmospheric aerosol consists of submicronic solid and liquid particles which exist in the air for at least a few days. Aerosol appears in the atmosphere as layers and clouds. Its origin can be natural (volcano eruptions, soil erosion, wavy motion of ocenas, *ets.*) or anthropogenic (burning or chemical processes, *etc*) [1]. Aerosols play very important part in air pollution, and physical and chemical processes in the atmosphere, through cloud formation as well as directly through sunlight attenuation. Aerosols cause cooling in the troposphere and heating in the stratosphere. A dense volcanic aerosol layer may have strong global climatic effects on radiative processes in the atmosphere by scattering and absorbing solar and terrestrial radiation and ozone destruction [2]. The fact that aerosol affects the light is used to study the properties of atmospheric aerosol component [3]. Due to additivity of scattering functions, in most measurements and experiments connected with atmospheric aerosol a single scattering is used. The size of scattering objects is such that we are usually deal-

ing with Mie's scattering. Classic Mie's scattering concerns spherical homogenous particles with radii comparable to the light wavelength [4]. It is extended also on more complex objects [5]. The scattered radiation field, produced by propagation of light beam in horizontal, vertical or slant direction in the atmosphere, can be essential source of information about aerosol. The elements of this field can be determined by using a solar radiometer, a transmission meter, a nephelometer or a lidar. The following parameters are usually determined from such measurements:

— The volume scattering (attenuation) coefficient or light or its integral over the sounding distances (optical thickness).

— The back-scattering coefficient or an angular dependence of scattering in specific spectral ranges (optical channels), instants of time, and points of space (a point, profile or layers).

The extinction coefficient α, equal to the volume scattering coefficient in the case of elastic scattering, is a total effective cross-section for scattering in a full solid angle, calculated per volume unit. The angular dependence of scattering P is defined as a differential cross-section for scattering calculated per volume unit and a solid angle unit at a direction forming the angle φ with the propagation direction of the original beam. The back-scattering coefficient β is the scattering matrix $P(\varphi)$ in a direction opposite to the propagation direction. The optical thickness of the atmosphere in vertical direction τ is an integral of the profile α over the height in a verical atmospheric column of thickness H [4]. There hold the following relations:

$$\alpha = \int_{4\Pi} P \mathrm{d}\omega, \quad \beta = P(\varphi = \pi), \quad \tau = \int_0^H \alpha(\alpha) \mathrm{d}h \tag{1}$$

where α is in km^{-1}, β in $\mathrm{km}^{-1}\mathrm{sr}^{-1}$, H in km.

2. Determination of scattering coefficients and aerosol optical thickness from optical sounding of the atmosphere

2.1. Determination of extinction coefficient α caused by aerosols from horizontal transmission measurements

To measure the extinction coefficient in near-ground layer of the atmosphere we use spectral transmission meters in which the light beam comes from a tungsten lamp, flash lamp or laser. This beam, formed by the optical system, is led in forizontal direction into the photometer located at a distance l, forming the measurement base (bistatic system) or prismatic mirror at a distance $l/2$, which reflects the beam to the photometer located nearby the source of light (monostatic system). The light beam is usually passed $2-5$ m above the ground or water level and its attenuation is the measure of turbidity of the sounded layer. The beam detectors are usually photomultipliers or photodiodes cooperating with telephoto lenses and the optical filter system. According to Bouger–Lambert's law, the transmission $T(l)$ of a layer with thickness l is described by the following formula [6]:

$$T(l) = \exp\left[-\int_0^l \alpha(z)\,dz\right]. \tag{2}$$

The atmosphere in horizontal direction at a distance of a few kilometers can be regarded as optically homogeneous and then the coefficient α for an optical channel of effective wavelengths λ can be calculated from the relation

$$\alpha(\lambda) = \frac{1}{l}\ln\left[T(\lambda)^{-1}\right]. \tag{3}$$

The extinction coefficient caused by aerosol α_A is calculated from the formula

$$\alpha_A(\lambda) = \alpha(\lambda) - \Delta\alpha(\lambda) \tag{3a}$$

where $\Delta\alpha(\lambda)$ is the correction for molecular extinction and absorption by atmospheric gaseous components.

2.2. Determination of vertical optical thickness τ of the atmosphere from the solar radiometer measurements

The total slant transmission of the atmosphere can be determined by direct solar radiation power measurement with a solar radiometer, based on known values of extraterrestrial solar power spectra density (solar constant). Because the atmosphere in a slant direction is highly inhomogeneous, this technique makes it possible to determine only the total optical thickness of vertical column of the atmosphere

$$\tau(\lambda) = \frac{1}{M}\ln\left[T(\lambda)^{-1}\right] \tag{4}$$

where M is the optical air-mass of the atmosphere which reduces data on measurement angle, optical hetergeneity and air pressure [7].

The aerosol optical thickness of the atmosphere $\tau_A(\lambda)$ is determined from

$$\tau_A(\lambda) = \tau(\lambda) - \Delta\tau(\lambda) \tag{4a}$$

where $\Delta\tau(\lambda)$ is the correction for optical thickness of atmospheric gaseous components.

1.3. Determination of profiles $\alpha(Z)$ and $\beta(Z)$ in the atmosphere from lidar soundings

Light radar (lidar) [8] records the signal coming from the trace of laser beam in the atmosphere caused by scattering. Because the beam has finite length of the order of several meters, the back-scattered radiation reaches the receiver from the successive sounding route intervals at successive moments of time and the signal is recorded as a function of distance Z, $U(Z)$. The beam of a properly chosen wavelength, running through the atmosphere, can only be scattered elastically on aerosols and air molecules. The signal recorded by the receiver, corrected for range-squared dependence $U(Z)$, is described by the equation [9]

$$U(Z) = C\left[\beta_A(Z) + \beta_M(Z)\right]\exp\left\{-2\int_0^Z\left[\alpha_A(z) + \alpha_M(z)\right]dz\right\} \tag{5}$$

where $U(Z) \equiv P(Z)Z^2$, $P(Z)$ is the power of the radiation received at a distance Z; C is the lidar constant. The subscripts "A" and "M" refer to coefficients for aerosol and air molecules, respectively.

Introducing symbols:

$$S_A(Z) = \alpha_A(Z)/\beta_A(Z), \quad S_M = \alpha_M(Z)/\beta_M(Z) \tag{6}$$

we can obtain the solution of lidar equation with respect to $\alpha_A(Z)$ or $\beta_A(Z)$, based on profile $U(Z)$, if we know the lidar ratio for aerosol $S_A(Z)$ and scattering values for the given atmosphere layer at a distance Z_0 [10], [11]. Values of $\alpha_M(Z)$, $\beta_M(Z)$ can be calculated from the atmosphere model [12]:

$$\beta_A(Z) = \cfrac{U(Z)\exp\{J(Z_0, Z, z)\}}{B(Z_0) - 2\int\limits_{Z_0}^{Z} S_A(z)U(z)\exp\{J(Z_0, z, ')\}\mathrm{d}z} - \beta_M(Z) \tag{7}$$

where:

$$B(Z_0) = \frac{U(Z_0)}{\beta_A(Z_0) + \beta_M(Z_0)}, \quad J(a, b, c) = -2\int\limits_{a}^{b}[S_A(c) - S_A]\beta_M(c)\mathrm{d}c.$$

Expression (7) is the solution of lidar equation in terms of $\beta_A(Z)$ and with the help of Eq. (6) we may obtain the profile of extinction coefficient $\alpha_A(Z)$.

3. Relation between single scattered radiation field components and microstructures of aerosol particles

Based on Mie's scattering theory [4], the relation between microstructure of scattering centers and single scattered radiation field components can be written as follows:

$$\mathrm{EXF}\,(\lambda, \varphi) = 2\pi \int\limits_{\varphi}^{} \int\limits_{a_1}^{a_2} K(a, \lambda, \varphi, m))\pi a^2\,\mathrm{d}N(a)\sin\varphi\mathrm{d}\varphi\mathrm{d}a \tag{8}$$

where EXF is one of the experimental functions: $\alpha(\lambda)$, $P(\lambda, \varphi)$ or $\beta(\lambda)$; a is the equivalent radius of speherical particle, K is the kernel of equation described by Mie's theory, λ -- the wavelength, φ — the scattering angle, m — the complex refractive index, $\mathrm{d}N(a)$ — the function describing particle number density per 1 cm^3, with radius $a \in (a, a + \mathrm{d}a)$, a_1, a_2 are ranges of particle radii.

A strict solution of integral Eq. (8) with respect to distribution function $\mathrm{d}N(a)$ based on measurement of $\alpha(\lambda)$, $\beta(\lambda)$ or $P(\lambda, \varphi)$ imposes requirements as to the wavelengths or scattering angles that are difficult to fulfil; moreover, such a solution is unstable and leads to cumulation of errors [13]. That is why attempts have been made to obtain approximate solutions based on iterative algorithms fit to experimental data the theoretical characteristics, for randomly selected aerosol models is based on Mie's scattering theory [14]. A good approximation describing the aerosol particle size distribution in the atmosphere is a multicomponent model, with components described by Gaussian logarithmic distributions with the number of

components $n \in (1, 4)$ [15]−[18]:

$$dN(a) = \sum_{i=1}^{n} dN(a) = \sum_{i=1}^{n} N_i f_i(a, a_0, A) da,$$

$$f_i(a, a_0, A) = 0.434 \sqrt{A/\pi} \, a^{-1} \exp\left[-A\left(\log \frac{a}{a_0}\right)^2 \right], \tag{9}$$

$$\int_0^{\infty} f_i(a, a, A) da = 1, \quad i = 1, \ldots, 4.$$

The total density of particles, *i.e.*, the number of particles per cubic centimeter, $N_3 \, [\text{cm}^{-3}]$, the total number of particles in atmosphere of cross-section of 1 cm^2, $N_2 \, [\text{cm}^{-2}]$, the mean modal radius $a_{\text{mm}} \, [\mu\text{m}]$ and the effective radius $a_{\text{eff}} \, [\mu\text{m}]$ are described by the formulae:

$$N_3 = \sum_{i=1}^{n} N_{3i}, \quad N_2 = \sum_{i=1}^{n} N_{2i},$$

$$a_{\text{mm}} = \frac{1}{N} \sum_{i=1}^{n} N_i a_{0i}, \quad a_{\text{eff}} = 3\frac{V}{S}, \quad V = \sum_{i=1}^{n} V_i, \quad S = \sum_{i=1}^{n} S_i, \tag{10}$$

$$V_i = \frac{4}{3}\pi N_i \int_0^{\infty} a^3 f_i(a, a_0, A) da, \quad S_i = 4\pi N_i \int_0^{\infty} a^2 f_i(a, a_0, A) da$$

were $n \leqslant 4$ is the number of fractions in multi-component model, V is the total particle volume concentration of aerosols [μm^3] per 1 cm^3 of air or in vertical atmosphere column in 1 cm^2 cross-section, S is the total particle surface-area concentration [μm^2] per 1 cm^3 of air or in vertical atmosphere column of 1 cm^2 cross-section.

The author has introduced the following synthetic relations between components of field-scattered radiation and parameters of aerosol model described by relations (9):

$$\alpha_{\text{AMOD}}(\lambda_j) = 10^{-3} \sum_{i=1}^{n} N_{3i} \, \bar{q}_i \, [f(a, a_0, A), m, \lambda_j],$$

$$\tau_{\text{AMOD}}(\lambda_j) = 10^{-8} \sum_{i=1}^{n} N_{2i} \, \bar{q}_i \, [f(a, a_0, A), m, \lambda_j],$$

$$\bar{q}_i(\lambda_j) = \pi a_{0i}^2 Q_{Gi,j}\left(\frac{2\pi a_{0i}}{\lambda_j}, A_i, m\right),$$

$$Q_{Gi,j}\left(\frac{2\pi a_{0i}}{\lambda_j}, A_i, m\right) = \frac{1}{a_{0i}^2} \int_0^{\infty} Q\left(\frac{2\pi a}{\lambda_j}, m\right) a^2 f_i(a, a_0 \, A) da,$$

$$\beta_{\text{AMOD}}(\lambda_j) = 10^{-3} \sum_{i=1}^{n} N_{3i} \, \bar{q}_{\varkappa i} \, [f(a, a_0, A), m, \lambda_j], \tag{11}$$

$$\bar{q}_{\pi i}(\lambda_j) = \pi a_{0i}^2 Q_{\pi Gi,j} \left[f(a, a_0, A), m, \lambda_j \right],$$

$$Q_{\pi Gi,j} = \frac{1}{a_{0i}^2} \int\limits_0^\infty I\left(\frac{2\pi a}{\lambda_j}, m, \varphi = \pi \right) a^2 f_i(a, a_0, A) \mathrm{d}a, \tag{11}$$

$j = 1, \ldots, k$, k is the number of optical channels.

The following symbols have been introduced:

N_{2i} [cm^{-2}] — the number of particles in the column of atmosphere of 1 cm^2 cross-section for the i-the model component.

N_{3i} [cm^{-3}] — the number of particles in 1 cm^3 of the atmosphere (particle number density for the i-the model component).

$\bar{q}_i [f(a), m, \lambda]$ [μm^2] — the average effective cross-section per particle for extinction for the i-th model component at wavelength λ.

$Q_{Gi}(a_0, A, \lambda, m)$ — average effciciency factor for extinction (ratio of the average cross-section for extinction per particle to geometrical cross-section per particle with a modal radius) for the i-th model component at wavelength λ.

$Q(a, \lambda, m)$ — the efficiency factor for extinction per particle with radius a and refractive index m at wavelength λ, according to Mie's theory [4].

$\bar{q}_{\pi i} [f(a), m, \lambda, \varphi = \pi]$ — the average cross-section for back- scattering per particle for the i-the model component at wavelength λ.

$Q_{\pi i}(a_0, A, \lambda, m, \pi)$ — the average efficiency factor for back-scattering for the i-the model component at wavelengt λ.

$I(a, \lambda, m, \varphi)$ — the scattering cross-section per particle in direction φ according to Mie's theory [4].

In order to determine the parameters describing the multi-component model of atmospheric aerosol (9) based on the measured scattering radiation field components $\alpha_A(\lambda)$, $\beta_A(\lambda)$ and $\tau_A(\lambda)$, special algorithms have ben developed. In these algorithms, the best fitting to experimental functions is searched (using the nonlinear least-squares method) through an analysis of theoretical characteristics obtained for randomly selected parameters out of the set of real values of the aerosol model. This technique is called randomized minimization search techique (RMST). The proces can be described by the following expression:

$$\sum_{j=1}^k \left[\mathrm{EXF}(\lambda_j) - \mathrm{MOD}_n(\lambda_j) \right]^2 \leqslant \varepsilon \tag{12}$$

where n is the number of a consecutive sampling; in place of $\mathrm{EXF}(\lambda_j)$ we put measured data $\alpha_A(\lambda_j)$, $\beta_A(\lambda_j)$ and $\tau_A(\lambda_j)$ and in place of $\mathrm{MOD}(\lambda_j)$ the respective expressions: $\alpha_{\mathrm{AMOD}}(\lambda_j)$, $\beta_{\mathrm{AMOD}}(\lambda_j)$ and $\tau_{\mathrm{AMOD}}(\lambda_j)$, (Eq. (11)). Parameter ε is the arbitrary small value of the fitting threshold. Upon reaching the fitting threshold, the iterative process stops. It is assumed that this way the randomly selected model parameters (Eq. (9)) describe the real atmospheric aerosol. The lidar sounding of the stratosphere that aims at studying the aerosol component of the atmosphere is, for technical reasons, carried out mostly at one or two wavelengths. They are in most cases the harmonic of YAG laser: 1064 and 532 nm. The results of soundings are

shown in a standard way as vertical profiles of the following quantities:

$$R_{T,M}(h, \lambda) = \frac{\beta_A(h, \lambda) + \beta_M(h, \lambda)}{\beta_M(h, \lambda)}, \tag{13}$$

$$R_{2,1}(h, \lambda_1, \lambda_2) = \frac{\beta(h, \lambda_2)}{\beta(h, \lambda_1)}, \tag{14}$$

$$\tau_A(h_1, h_2, \lambda) = \int_{h_1}^{h_2} \beta_A(h, \lambda) S_A(h) dh \tag{15}$$

where $R_{T,M}$ is the ratio of the total back-scattering coefficient to the molecule back-scattering coefficient, $R_{2,1}$ is the back-scattering ratio at two wavelengths, $\lambda_2 = 1064$ nm and $\lambda_1 = 532$ nm, and S_A is the lidar ratio for aerosoles (see Eq. (6)). A step ahead in presenting the results of lidar sounding, *e.g.*, as vertical concentration profiles, causes a great trouble. To determine the parameters of two-component model based on sounding for two wavelengths one must adopt strong assumptions as to physical characteristics of aerosol, make additional measurements (*e.g.*, the signal depolarization coefficient) or increase the number of measured wavelengths. For instance, in the stratosphere disturbed by strong volcanic eruption, which took place on June 15, 1991 at Pinatubo, during the following first dozen of months there was a strong aerosol transformation, converting the water vapour and sulfur dioxide into sulfuric acid molecules and the change of stratification of liquid and solid components of aerosol. This caused a big change of mean aerosol refractive index and aerosol stratification. The modelling of stratospheric aerosol was then very difficult and was made with the help of *in situ* balloon measurements [17]. A few years after the strong volcano eruption the homogenization of physical characteristics of aerosol takes place and the total aerosol contents in the stratosphere strongly decreases (the aerosol falls down into the troposphere), reaching the background level during a few years. In the stratosphere which is disturbed by a strong volcano eruption, the two-component model (confirmed by balloon measurements *in situ*) is proper for describing aerosol, while for background the mono-component model gives a satisfactory description [18]. In the case of mono-component model, the parameters of the model and values obtained from measurements (see Eqs. (13) and (14)) can be related in a very probable way as follows:

$$a_0(h) = F_1[R_{2,1}(h), A(h), m(h)],$$
$$\bar{q}_{back}(\lambda, h) = F_2[\lambda, a_0(h), A(h), m(h)], \tag{16}$$
$$\beta_A(\lambda, h) = 10^{-3} N_3(h) \bar{q}_{back}[\lambda, a_0, (h), A(h), m(h)]$$

where F_1, F_2 are the functionals which can be determined theoretically, $\beta_A(\lambda, h)$ can be determined from $R_{T,M}$ (Eq. (13)) based on the known atmosphere model, vertical profile of air density [12] and active cross-section for attenuation of air molecule from Rayleigh's scattering thoery [8]. If we know the profile of refctive index $m(h)$ or $m(h) = $ const., then expressions (16) can be the basis for determining concentration profile $N_3(h)$.

4. Examples of measurement results

In Figure 1 we present the extinction coefficient as a function of wavelength in visible range and near-infrared measured by 6-channel transmission meter with tungsten lamp under the conditions of light haze. The unique measurements made by the author in 1967 [16] are now interpreted again using the RMST method. The obtained size distributions of aerosol radii for 8 bands of meteorological visibility are shown in Fig. 2. For haze there dominate particles of radii from 0.2 to 0.4 μm with admixture of bigger particles of radii from 0.7 to 0.9 μm. In Figure 3 we present the plot of particle number density N, mean modal particle radius a_{mm}, and effective
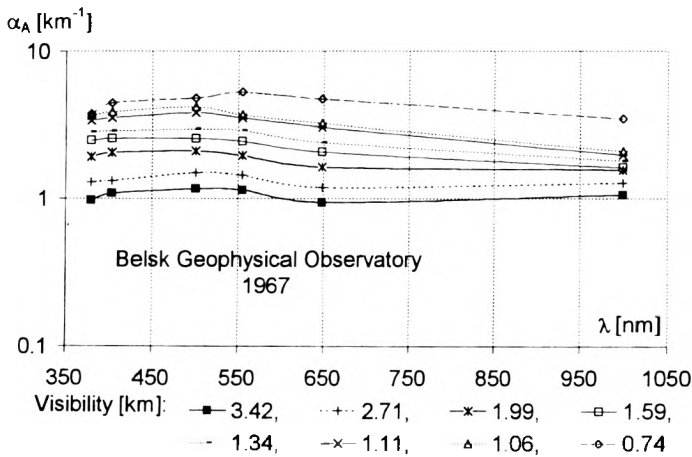
Fig. 1. Extinction coefficients vs. wavelengths for haze at different visibilities. Soundings for 200 m distance, 2 m above ground at Belsk Geophysical Observatory.
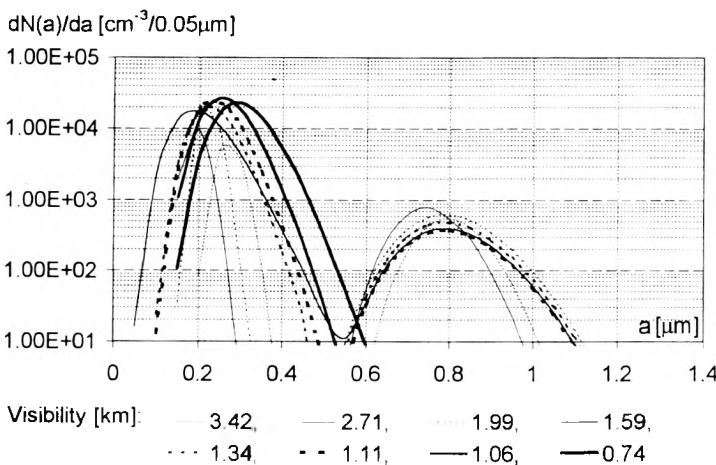
Fig. 2. Aerosol distribution in haze calculated by means of RMST algorithm (the randomized minimization search technique) from $\alpha_A(\lambda)$ presented in Fig. 1.
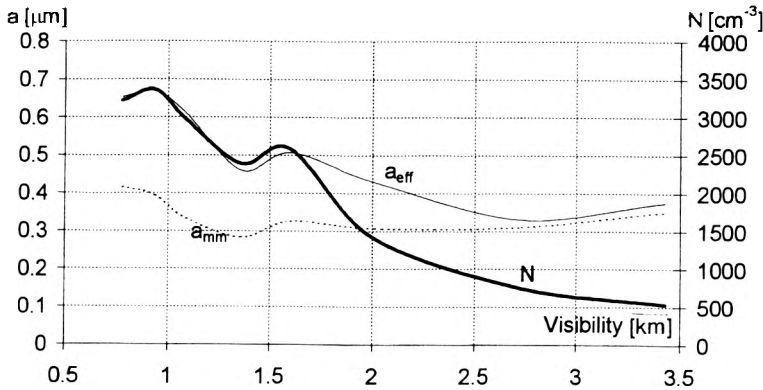
Fig. 3. Particle radii a_{eff}, a_{mm} and aerosol concentration N vs. visibility calculated from $\alpha_A(\lambda)$ presented in Fig. 1.
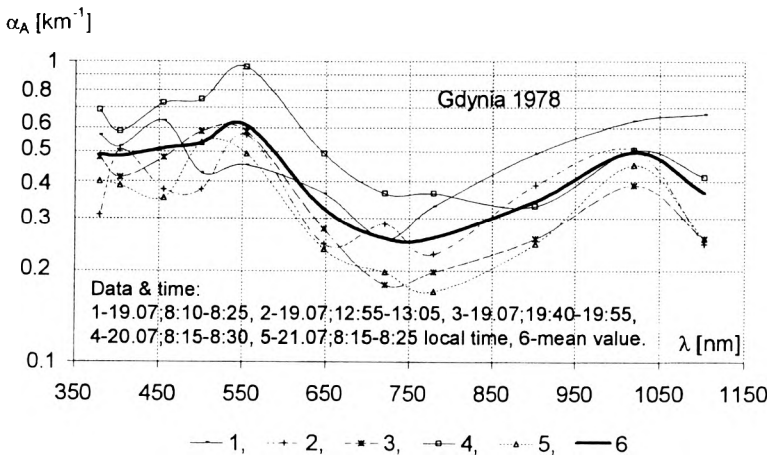

Fig. 4. Extinction coefficient for marine aerosols vs. wavelengths sounded for 1450 m distance, 5 m above water level at Baltic Sea in Gdynia. Curves 1−5 are results of independent measurements, curve 6 represents the mean value.

particle radius α_{eff}, as a function of visibility. Transition from haze to fog (a decrease in visibility below 1 km) can be caused by both a condensative increase in size of bigger particles fraction (increase of a_{mm} and a_{eff}) and an increase of concentration N of small particles fractions, and this latter mechanism seems to dominate. In Figure 4, we show the results of mesurements of extinction coefficient versus wavelength made by the author with the use of 11-channel transmission meter with flash lamp in a near-water layer at the Baltic Sea (made in Gdynia, Poland, in 1978, not published yet). The results of measurements processed with the RMST method are shown in Fig. 5. The average distribution for 5 measurement series made at mean visibility conditions is expressed by 3-component model and its character differs significantly from that of the distribution for continental haze shown in Fig. 2.
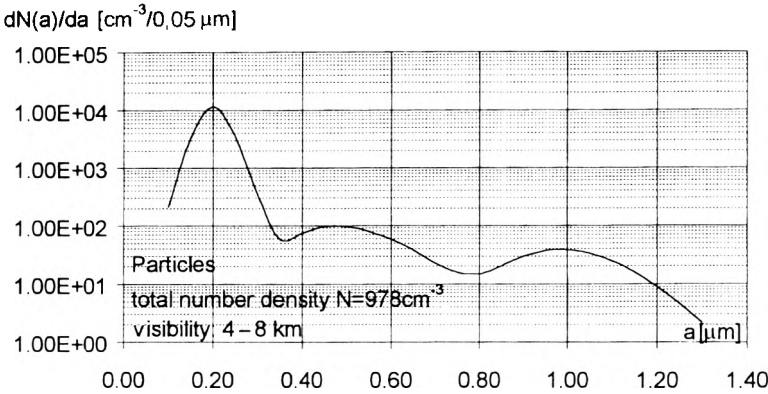
dN(a)/da [cm^{-3}/0,05 µm]

Fig. 5. Marine aerosol size distribution calculated by means of RMST algorithm from mean value $\alpha_A(\lambda)$, presented in Fig. 4 (curve 6).
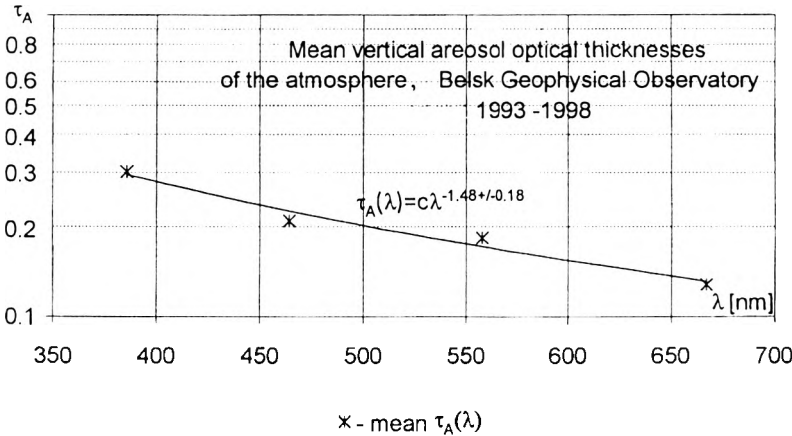

✕ - mean $\tau_A(\lambda)$

Fig. 6. Five-year mean vertical aerosol optical thickness τ_A vs. wavelengths measured at Belsk Geophysical Observatory in the period from June 1993 through May 1998 by means of sun radiometer. Data fit exponential Angstrom's formula with exponent 1.48 ± 0.18.

In Figure 6, we present the average 5-year mean vertical aerosol optical thickness of the atmosphere τ_A versus wavelength for visible range. The measurements by means of 4-channel solar radiometer (Linke actinometer) according to the author's design have been made in 1993–1998 at Belsk Geophysical Observatory. These results confirm the well-known regularity that the average dependence of atmosphere extinction on wavelength in visible range is described by exponential Angstrom's formula with exponent of 1.3 ± 0.6 [19].

In Figure 7, we show examples of different particle size distributions for average monthly $\tau_A(\lambda)$ values and the distribution for 5-year average $\tau_A(\lambda)$ values, obtained by the RMST method. The average monthly distributions of particle sizes can significantly differ from each other. In few cases, in atmosphere column over Belsk

dN(a)/da [cm^{-2}/0.05 µm]

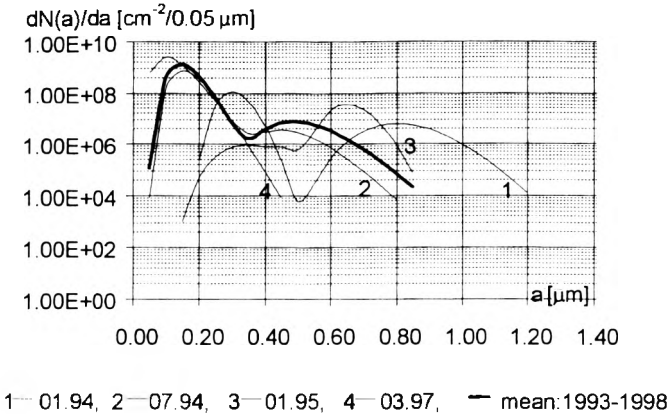1 — 01.94, 2 — 07.94, 3 — 01.95, 4 — 03.97, — mean:1993-1998

Fig. 7. Examples of mean monthly aerosol size distributions, and five-year mean aerosol size distribution, obtained by means of RMST algorithm from measured $\tau_A(\lambda)$ data at Belsk Geophysical Observatory in 1993 – 1998.

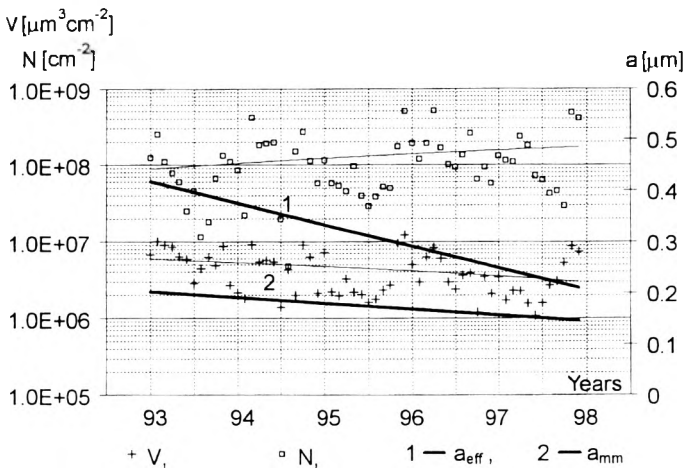+ V,   □ N,   1 — a_{eff},   2 — a_{mm}

Fig. 8. Five-year trend of V, N, a_{eff} and a_{mm} calculated by means of RMST algorithm from measured $\tau_A(\lambda)$ values at Belsk Geophysical Observatory in 1993 – 1998.

Geophysical Observatory there dominated big particles, of $0.6 - 1.2$ µm radii (curves 1 and 3, in Fig. 7). However, in most cases, small, $0.15 - 0.30$ µm, particles (curves 2 and 4) dominated which has its impact on the average distribution during 5 years (the curve "mean" in Fig. 7).

In Figure 8, we show 5-year trends (1993 – 1998) of average monthly values of the following quatities: N, V, a_{eff} and a_{mm}. In this period we observe $9.8 \pm 3.9\%$ decrease of the total particle volume concentration V, $18.6 \pm 11.7\%$ increase of the number density concentration N, $9.9 \pm 2.3\%$ decrease of the effective radius a_{eff}, and $5.5 \pm 3\%$ decrease of the mean modal radius a_{mm} per year. This can be explained as follows: in this period "cleaning of the troposphere" took place, caused by the reduction
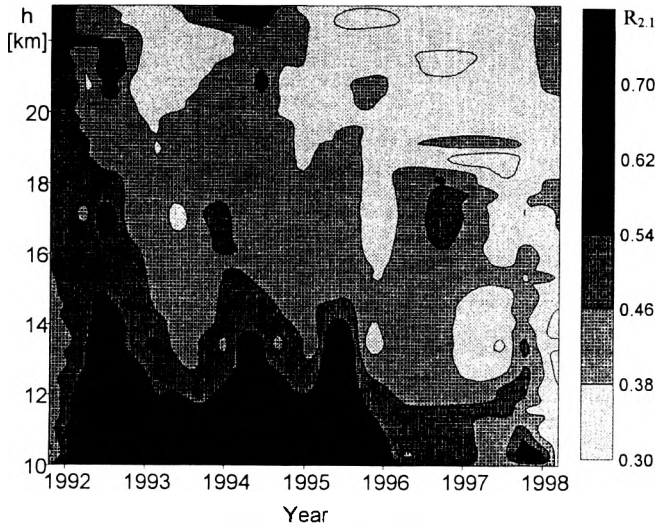
Fig. 9. Ratio $R_{1,2} = \beta_A(\lambda_2, h)/\beta_A(\lambda_1, h)$ of aerosol back-scattering coefficients at two wavelengths, $\lambda_2 = 1064$ nm and $\lambda_1 = 523$ nm, vs. altitude h [km] measured by means of lidar.
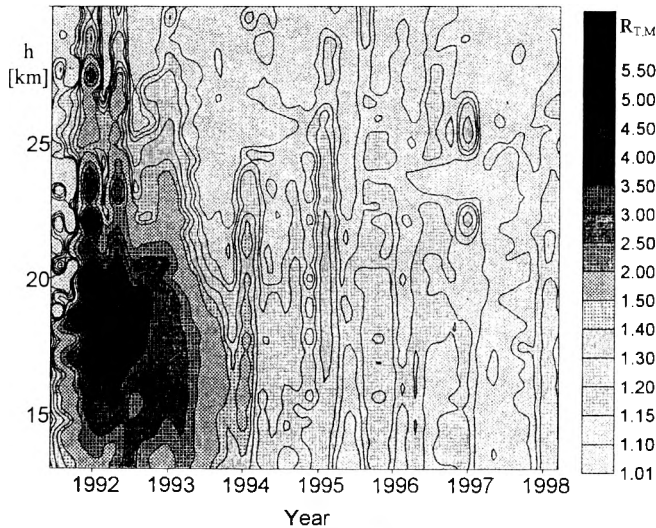

Fig. 10. Ratio $R_{T,M} = [\beta_A(\lambda_1, h) + \beta_M(\lambda_1, h)]/\beta_M(\lambda_1, h)$ of the total back-scattering coefficient to molecular back-scattering coefficient vs. altitude h [km] measured by means of lidar.

of anthropogenic aerosol emission (change of industry technology and energy sources in Poland). The troposphere aerosol which is the main factor contributing to vertical atmospheric extinction was subject to deep transformation towards the smaller particles and though its N concetration was increasing, the a_{mm} and a_{eff} radii were decreasing significantly along with a decrease of V concentration proportional to the weight concentration.

In Figures 9 and 10, we show the plots of scattering ratio at two wavelengths $R_{1,2}$ (Eq. (14)) and the ratio of the total back-scattering coefficient to the molecular back-scattering coefficient $R_{T,M}$ ($\lambda = 532$ nm), (Eq. (13)), which was possible due to international cooperation: the measurements were made at the Minsk lidar station in Byelorussia (lat. 53.85 N, long. = 27.5 E) throughout seven years (1992—1998) [20] and since 1996 also at the lidar station of Belsk Geophysical Observatory (see Appendix). Morphological analysis of parameters $R_{1,2}$ and $R_{T,M}$ presented in Figs. 9 and 10 shows the progressive decrease of their values since the Pinatubo eruption (June 15, 1991) and the descent of stratospheric aerosol patches into the troposphere. An attempt at evaluating the quantitative changes in the stratosphere can be undertaken based on expressions (16). One can try to evaluate the N concentration for a specified altitude and a moment of time.
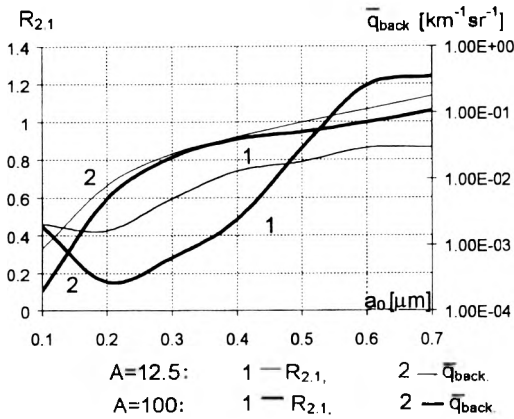

Fig. 11. Modal radius a_0 [μm] vs. ratio $R_{2,1}$ and mean cross-section for back-scattering $\bar{q}_{back}(\lambda, a_0, A, m = 1.50)$ vs. modal radius, calculated for monomodal log-Gauss model of aerosols (Eq. 9)), for two values of parameter A: 12.5 and 100.
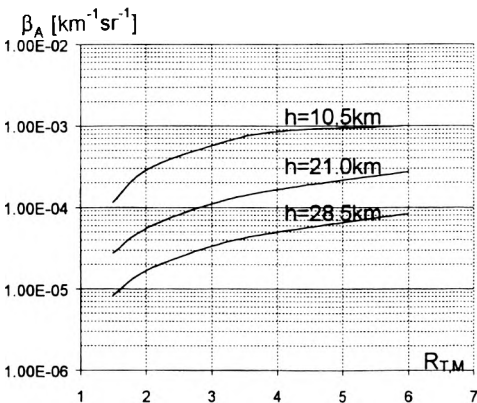

Fig. 12. Back-scattering coefficient for aerosols $\beta_A(\lambda_1, h)$ vs. ratio $R_{T,M}(\lambda_1, h)$ calculated for three altitudes: 10.5 km, 21.0 km and 28.5 km and the Standard Model of the Atmosphere.

In Figure 11, we show graphically the functionals F_1 and F_2 (Eq. (16)) calculated for mono-component aerosol model with the parameters: $a_0 \in (0.1, 0.7)$, $A = 12.5$ and $A = 100$, and $m = 1.50$, at wavelength $\lambda = 532$ nm.

In Figure 12, we show the dependence of β_A on $R_{T,M}$ at various altitudes, calculated for Standard Model of the Atmosphere [12]. For example, if we have the measured values $R_{2,1} = 0.5$ and $R_{T,M} = 3$ and take the distribution parameter $A = 100$, the modal radius $a_0 = 0.4$ μm and the corresponding mean effective back scattering cross section $\bar{q}_{back} = 0.039$ km^{-1} sr^{-1} (Fig. 11), we obtain for $\beta_A(h, \lambda = 532$ nm) the following values for 3 different altitudes:

$\beta_A(10.5$ km$) = 5.56 \cdot 10^{-4}$ km^{-1} sr^{-1},

$\beta_A(21.0$ km$) = 1.09 \cdot 10^{-4}$ km^{-1} sr^{-1},

$\beta_A(28.5$ km$) = 3.32 \cdot 10^{-5}$ km^{-1} sr^{-1}.

The corresponding N concentrations are:

$N(10.5$ km$) = 14.5$ cm^{-3},

$N(21.0$ km$) = 2.8$ cm^{-3},

$N(28.5$ km$) = 0.9$ cm^{-3}.

The decrease of $R_{2,1}$ is equivalent to the decrease of modal radius of the distribution and the decrease of $R_{T,M}$ is equivalent to the decrease of N concentration.

A quantitative and qualitative analysis of changes in profiels $R_{2,1}$ and $R_{T,M}$ with time gives evidence for the "cleaning" processes in the stratosphere observed after the Pinatubo eruption: a decrease in size of the particles and in their N concentration caused by aerosol transformation and its descent to the troposphere. The results of measurements and thier analysis presented here show the potential of optical soundings based on Mie's and Rayleigh's elastic scatterimg in the study of the aerosol components in the atmosphere.

Appendix

Lidar of the Geophysical Observatory at Belsk, Poland
(lat. 51°50′ N, long. 20°47′ E, $h = 188$ m above sea level)

Specification of the lidar system

Transmitting system:

Laser 1	Nd:YAG	
Wavelengths	1064 nm,	532 nm
Power	100 mJ pp,	25 mJ pp
Pulse width	10 ns,	10 ns
Repetition rate	20 Hz,	20 Hz
Collimator ø	10 cm,	10 cm
Laser 2	Ruby	
Wavelength	694.3 nm	
Power	500 mJ pp	
Pulse width	20 ns	
Repetition rate	0.08 Hz	
Collimator ø	10 cm	

Detecting system:

Telescope ⌀	50 cm (Cassegrain type)
Filters (half width)	532−1.5 nm, 694.3−1.5 nm, 1064−4.0 nm
Photomultipliers	532-FEU-140, 694.3-FEU-84, 1064-KOMETA (all made in Russia)
Photon counters	2 × MCA (multichannel analyzer) 1064 ch.
	Counting the number of photons within each channel
	(1 channel = 0.8 μs)
Analog signal recorders	2 × ADD 1024 channels (1 channel = 100 ns)

References

[1] JUNGE C. H., *Air Chemistry and Radiaactivity*, Academic Press, New York, London 1963.

[2] HAYASAKA T., IWASAKA N, HASHIDA G., TAKIZAWA I., TANAKA M., Geophys. Res. Lett. **12** (1994), 1137.

[3] ZUJEV V. E., KABANOV M. V., *Optica atmosfernogo aerozola*, (in Russian), [Ed.] Gidrometeoizdat, Leningrad 1987.

[4] VAN DE HULST H. C., *Scattering by Small Particles*, Wiley, New York 1957.

[5] KERKER M., *The Scattering of Light and Other Electromagnetic Radiation*, Academic Press, New York, London 1969.

[6] MIDDLETON W. E. K. *Vision Through the Atmosphere*, University of Toronto Press, 1952.

[7] STETTLER M., VON HOYNINGEN-HUENE W., Beitr. Phys. Atmosph. **66** (1993), 347.

[8] HINKLEY E. D., *Laser Monitoring of the Atmosphere*, Topics in Applied Physics, Vol. 14, Springer-Verlag, Berlin, Heidelberg, New York 1976.

[9] KLETT J. D., Appl. Opt. **20** (1981), 211.

[10] PUCHALSKI S., Acta Geophys. Pol. (in Polish), **1** (1975), 15.

[11] SASANO Y., BROWELL V., ISMAIL S., Appl. Opt. **24** (1985), 3929.

[12] MCCLATCHEY A., D'AGATI P., *Atmospheric Transmission of Laser Radiation*, Report No. AFGL-TR-78-0029, Air Force Geophysics Laboratory, Massachusetts 01731, 1978.

[13] BAKHTIYAROV V. G., FOITZIK L., PERELMAN A. Y., SHIFRIN K. S., Pure Appl. Geophys. **64** (1966), 204.

[14] HEINTZENBERG J., MULLER H., QUENZEL H., THOMALLA E., Appl. Opt. **20** (1981), 1308.

[15] FOITZIK L., SPANKUCH D., Z. Meteorol. **21** (1969), 136.

[16] PUCHALSKI S., *Particle size distribution of aerosols in the ground air layer in pre-fog stages determined by measurement of horizontal transmisssion of light*, Publ. Inst. Geophys. Pol. Acad Sci., D-22, 1971.

[17] WANDINGER U., ANSMANN A., REINCHARDT J., DESHLER T., Appl. Opt. **34** (1995), 8315.

[18] WANG P. H., KENT G. S., MCCROMICK M. P., THOMASON L. W., YUE G. K., Appl. Opt. **35** (1996), 433.

[19] WOODMAN D. F., Appl. Opt. **13** (1974), 2193.

[20] CHAIKOVSKY A. P., IVANOV A. P., OSIPENKO F. P., SHCHERBAKOV V. N., KOROL M. M., PUCHALSKI S., SOBOLEWSKI P., *Investigation of stratospheric aerosol layer temporal changes with two-wavelengths lidar*, Fifth Intern. Symp. on Atmospheric and Ocean Optics, June 15−18, 1998, Tomsk, Russia, SPIE **3583** (1999), 452.